Catalysis Today 201 (2013) 49–56

Contents lists available at SciVerse ScienceDirect

Catalysis Today

journal homepage: www.elsevier.com/locate/cattod

# Catalytic wet air oxidation of pentachlorophenol over Ru/$ZrO_2$ and Ru/$ZrSiO_2$ catalysts

Huangzhao Wei[a,b], Xiaomiao Yan[a], Songbo He[a], Chenglin Sun[a,*]

[a] Dalian Institute of Chemical Physics, Chinese Academy of Sciences, Dalian 116023, PR China
[b] Graduate University of Chinese Academy of Sciences, Beijing 100049, PR China

ARTICLE INFO

Article history:
Received 14 January 2012
Received in revised form 2 July 2012
Accepted 3 July 2012
Available online 9 August 2012

Keywords:
Catalytic wet air oxidation
Pentachlorophenol
$ZrSiO_2$
$ZrO_2$
Kinetics

ABSTRACT

$ZrSiO_2$ and $ZrO_2$ supports loaded with active component Ru were unprecedentedly evaluated in catalytic wet air oxidation reaction of pentachlorophenol (PCP). The study results showed that the specific surface area of $ZrSiO_2$ which was prepared by high temperature aging method was much larger than that of $ZrO_2$, and it performed a better catalytic activity in catalytic wet air oxidation after being loaded with Ru. When the initial concentration of PCP was 125 mg $L^{-1}$, PCP conversion reached 92% after 90 min under the low temperature and pressure conditions of 180 °C and 0.1 MPa oxygen partial pressure. PCP conversion was increased by raising reaction temperature, increasing oxygen partial pressure, reducing the initial concentration of PCP and prolonging reaction time. The kinetics study of PCP in catalytic wet air oxidation showed that the catalytic wet air oxidation reaction of PCP obeyed first order kinetic model and its Arrhenius activation energy was 96.98 kJ $mol^{-1}$. The main intermediates of PCP in CWAO were acetic acid, oxalic acid and chlorine ion.

## 1. Introduction

Since the 1930s, pentachlorophenol (PCP) is widely used as wood preservatives, fruit trees pesticides or bactericide, whose sodium salt is utilized as the medicine of killing oncomelania to cure schistosomiasis. The properties of PCP are relatively stable, and it is difficult to be degraded by using conventional wastewater treatment methods such as physical, chemical and biological methods [1,2]. Besides, PCP has serious carcinogenic, teratogenic and mutagenic effects. PCP has already been included in the blacklist of priority pollutants, environmental endocrine disruptors and persistent organic pollutants. Therefore, it is very important to develop a safe and effective treatment technology of PCP.

Today, the treatment methods of PCP are mainly physisorption [3,4], biodegradation [5,6] and advanced oxidation process [7–11] at home and abroad. Physisorption only transfers pollutants from the aqueous phase to the surface of adsorbents. In fact, it does not eliminate pollutants. Biodegradation has several disadvantages, such as the long time of the treatment, the large area of devices taking up, the bad treatment effect and easily influenced by seasons. Advanced oxidation processes (AOPs) possess the advantages of quick degrading rate and no secondary pollution and so on, so they are increasingly employed to treat PCP wastewater. The common methods of AOPs used to treat PCP include photo-catalytic oxidation process [7], supercritical oxidation process [8], ozonation oxidation process [9], Fenton's oxidation process [10] and electro-catalytic oxidation process [11]. In AOPs, catalytic wet air oxidation (CWAO) has many merits, including simultaneous treatment of chemical oxygen demand (COD) and removal of nitrogen and sulfur compounds in one stage, low running cost, a compact plant design for low space requirements, stably continuous and automatic operation, deodorization and decolorization, the process is extremely clean because it does not involve the use of any harmful chemical reagents and the final products (if complete oxidation is achieved) are carbon dioxide and water, no secondary pollutants like sludge and ashes, the wastewater with COD of about 20,000 mg/L may be treated without supplying any auxiliary fuel, the wastewater treated by CWAO may be reused and the steam from the oxidation reaction of the wastewater may be recycled into energy. Consequently, it is utilized to treat all kinds of organic wastewater [12–14]. However, there has not been a report about the PCP treatment by using CWAO.

$ZrO_2$ is increasingly used as a support in catalyst. It has several useful properties that favor its application in catalysis. Among the physical properties that make it being a useful support under harsh conditions are its high melting point of 2370 °C, low thermal conductivity, and high corrosion resistance [15]. $ZrO_2$ does not dissolve in the acidic and alkaline solution, which makes it a good catalyst support in CWAO reactions. The common methods for the preparation of $ZrO_2$ include direct calcination method [16],

---

* Corresponding author. Tel.: +86 411 84379326; fax: +86 411 84699965.
E-mail addresses: weihuangzhao@qq.com, clsun@dicp.ac.cn (C. Sun).

http://dx.doi.org/10.1016/j.cattod.2012.07.004

precipitation method [17], azeotropic distillation method [18], hydrolysis method [19], sol–gel method [20], reversed phase micro-emulsion method [21], vapor phase hydrolysis at lower temperature and extraction separation method used to prepare $ZrO_2$ for nuclear industry. Chuah and co-workers [22] found that the digestion of the hydrous oxide may increase the thermal stability of the resulting $ZrO_2$. Sato et al. [23] and Miller et al. [24] found that silica dissolving in the solution from the glass vessel and re-depositing on the zirconium hydroxide during the digestion process was the main factor of high specific area $ZrO_2$.

Catalysts containing noble metals exhibit usually higher activity than base metal catalyst in CWAO reaction, particularly in respect to carboxylic acids. Leaching of precious metals from CWAO catalysts has not been reported [25]. In precious metal catalysts, Ru is much cheaper than the other platinum group noble metals, so it has been studied by many scholars [26–28].

In this paper, $ZrO_2$ was prepared by precipitation method (PM) and hydrolysis method (HM), and $ZrSiO_2$ was prepared by deposition of silicate species on zirconia under hydrothermal conditions in aqueous ammonia. Then all of them were loaded with active component Ru and used to treat PCP in the autoclave. The effects on the conversion of PCP from temperature, oxygen partial pressure, the initial concentration of PCP, reaction time and PCP reaction kinetics in CWAO were studied.

## 2. Experimental

### 2.1. Reagents

Ruthenium Trichloride (37%Ru) was supplied by Shanghai Iridium Grain Plant. Zirconium(IV) oxychloride octahydrate (99.0%) and PCP (98.5%) were supplied by Sinopharm Chemical Reagent CO., Ltd. Ammonia solution (25.0%) was supplied by Tianjin Kermel Chemical Reagent Co., Ltd.

### 2.2. Analytical methods

Liquid samples taken from the reactor were analyzed by routine laboratory analyses, which were filtrated with 0.45 μm film to remove any catalyst particles and solid residue. The total amount of the organic substances in the aqueous phase was determined by measuring the chemical oxygen demand (COD). The COD values of the samples were determined by GB 11914-89 potassium clichromate methods. PCP concentration was analyzed via high performance liquid chromatography (HPLC). The HPLC system produced by Dalian Elite Analytic Instruments Co., Ltd. was equipped with an Elite C18 chromatographic column (4.6 mm × 250 mm, 5 μm) and a UV-detector set at 320 nm. The mobile phase was methanol: ammonium acetate ($2\,g\,L^{-1}$) = 85:15 (v/v) and the flow rate was fixed at $1.0\,ml\,min^{-1}$.

Typically a 50 ml sample containing PCP and organic reaction products was acidified to pH < 2 with concentrated $H_2SO_4$ solution, and then extracted twice using a total volume of 110 ml chloroform and methanol at the ratios of 0.9:1:1 (v/v/v for sample/chloroform/methanol). The combined extract was concentrated to 2 ml using a gentle stream of $N_2$ gas. The extract was stored at −10 °C until analysis.

Extracted samples containing PCP, intermediates, and byproducts were analyzed using a gas chromatograph (GC) (Agilent Technologies 7890A) equipped with a capillary column (HP-5ms, 30 m × 0.25 mm × 0.25 μm, Agilent J&W GC Columns) and a flame ionization detector (FID). A split injection of 5:1 was used with the oven temperature programmed as follows: 45–60 °C at 5 °C/min, 60 °C for 1 min, 60–210 °C at 3 °C/min, 210–300 °C at 20 °C/min. The injection temperature was 200 °C. The Detector temperature was 300 °C.

The carboxylic acid and $Cl^{-1}$ were analyzed via ion chromatography (IC). The ICS-3000 system produced by DIONEX was equipped with an AS11-HC chromatographic column (4 mm × 250 mm). The temperature of column and cell heater was 30 and 35 °C, respectively. The mobile phase was $30\,mol\,L^{-1}$ NaOH solution and the flow rate was fixed at $1.2\,ml\,min^{-1}$.

### 2.3. Catalytic wet air oxidation experiments

The reactions were performed in a 250 ml or 500 ml batch reactor equipped with a magnetically driven stirrer and an electric heating jacket. The reactor was CJF-0.25 or CJF-0.5 type autoclaves made of titanium alloy supplied by Dalian Tongda Autoclave Plant. 2.03 g PCP and 6.5 g NaOH were added into 1 L deionized water to prepare $2000\,mg\,L^{-1}$ PCP solution. In the standard procedure for a CWAO experiment, 0.1 g catalyst and 100 ml PCP solution were put into the 250 ml autoclave. The autoclave was closed, filled with a certain pressure of oxygen (0.1–2.1 MPa) and checked whether it was leak-free or not, then the heating-up program started. When the set temperature was attained, the stirrer started at a speed of 600 rpm. This time was taken as the zero time of reaction and the reaction time was set as 90 or 120 min. When the sample needed taking during the reaction, 250 ml autoclave was changed into 500 ml to do the experiment. The amount of both the catalyst and model compound solution was doubled. The liquid samples were periodically withdrawn from the reactor, filtered to remove any catalyst particle and finally analyzed.

Experiments were carried out at temperatures ranging from 135 °C to 195 °C and oxygen partial pressures ranging from 0.1 to 2.1 MPa. When the effect of the initial concentration of PCP on PCP conversion was studied, the experiment was carried out after diluting the prepared PCP solution.

The catalyst life evaluation test of 48 h was carried out in a fixed-bed reactor with upflow of PCP wastewater and air. The reaction condition was as follows: reaction temperature = 180 °C, reaction pressure = 2.0 MPa, catalyst dose = 10 ml, $V_{liquid} = 0.33\,ml\,min^{-1}$, $V_{gas} = 40\,ml\,min^{-1}$.

### 2.4. Catalyst preparation

#### 2.4.1. $ZrO_2$-PM

$ZrOCl_2$ solution ($0.3\,mol\,L^{-1}$) was added into $5\,mol\,L^{-1}$ ammonia solution drop by drop. The preparation was aged for 12 h at room temperature, filtrated under vacuum, washed with 1% dilute ammonia solution to no $Cl^{-1}$ in it which was detected with 1% $AgNO_3$ solution and washed with deionized water at last. The filter cake was respectively dried for 12 h at 50 °C and 100 °C. Then it was grinded with an agate mortar to sift through a 60 mesh sieve. At last, it was calcined at 500 °C for 2 h in a muffle furnace.

#### 2.4.2. $ZrO_2$-HM

$ZrOCl_2$ solution ($0.1\,mol\,L^{-1}$) was boiled for 96 h in a round-bottomed flask with a reflux device. The preparation was aged for 12 h at room temperature and boiled to a paste. The post treatment of the paste was as the same as the $ZrO_2$-PM.

#### 2.4.3. $ZrSiO_2$

$ZrOCl_2$ ($0.3\,mol\,L^{-1}$) solution was added into ammonia solution ($5\,mol\,L^{-1}$) drop by drop. The preparation was digested for 96 h at 100 °C. The silica was dissolved from the glass round-bottomed flask and re-deposit on the zirconia precipitate during the high temperature aging process. The post treatment was as the same as the $ZrO_2$-PM.

Ru was introduced by incipient wetness impregnation using aqueous solutions of ruthenium trichloride. To facilitate any comparison, the Ru content in all catalysts was fixed at 1 wt.%. After impregnation, the preparations were dried under vacuum for 2 h at 60 °C. At last, they were calcined at 350 °C for 6 h in a muffle furnace and labeled Ru/$ZrO_2$-PM, Ru/$ZrO_2$-HM and Ru/$ZrSiO_2$.

### 2.5. Catalyst characterization

#### 2.5.1. BET surface area

The specific surface area of $ZrO_2$ was assessed by $N_2$ adsorption isotherms at 77 K using QUADRASORB SI instrument produced by Quantachrome Company. The catalyst samples prior to the adsorption measurement were degassed at 300 °C for 3 h under vacuum. The specific surface area was obtained by $N_2$ adsorption isotherms and BET equation.

#### 2.5.2. XRD

Specimens were prepared by packing the powder samples in a glass samples holder. The X-ray diffraction (XRD) spectra of the support was obtained with X'Pert PRO instrument produced by PANalytical. The measurements were recorded in the $2\theta$ range of 10–90°.

#### 2.5.3. TPR and CO chemisorption

The interaction between $RuO_x$ and support was studied by temperature-programmed reduction (TPR) using a Micromeritics Auto-Chem II 2920 apparatus (American). Prior to the measurement, the samples were pretreated in Ar (99.99%, 20 ml $min^{-1}$) at 120 °C for 2 h. After cooling to room temperature in Ar, the gas flow was switched to 10% $H_2$ in Ar and the samples were heated from 50 °C to 300 °C with a temperature ramp of 10 °C/min. The hydrogen consumption was determined by a thermal conductivity detector. After the TPR experiment, CO chemisorption was determined at 50 °C in a 20 ml $min^{-1}$ stream of He using a pulsed-chemisorption technique, in which 0.1 ml CO/He (CO: 5 vol.%) pulses of each gas were utilized. After the CO chemisorption, transmission electron microscopy was determined.

#### 2.5.4. TEM

Transmission electron microscopy (TEM) images were obtained using a HT7700 operated at 100 kV. The images were used to determine the particle size of the Ru metal. The samples were ground in an agate mortar to fine particles and then dispersed ultrasonically in ethanol. The sample was deposited on a Cu grid covered by a holey carbon film.

#### 2.5.5. TGA

The weight loss mechanism of $ZrSiO_2$ precursor was studied by thermogravimetric analysis instrument supplied by Sygate. The sample about 200 mg was heated from room temperature to 800 °C at a heating rate of 3 °C $min^{-1}$ in an air flow of 50 ml $min^{-1}$.

#### 2.5.6. XRF

XRF was used to determine Silicon content in the $ZrO_2$ sample with Magix 601 equipment produced by PANalytical. The performing of each sample (1.5 g) was proceeded under 30 MPa condition for the XRF measurement.

## 3. Results and discussion

### 3.1. Characterization

#### 3.1.1. BET

As shown in Table 1, the specific surface areas of $ZrO_2$-PM and $ZrO_2$-HM were low and near, while $ZrSiO_2$ possessed four times higher specific surface area than $ZrO_2$-PM. This phenomenon indicated that the high specific surface area $ZrO_2$ reported by Chuah and Jaenicke [29] was caused not by the removal of defects in the $ZrO_2$ particles through the dissolution–deposition of $ZrO_2$, but by $SiO_2$ (5.29%) coating the wet $ZrO(OH)_2$ precipitates. The silica may dissolve from the glass round-bottomed flask and re-deposit on the zirconia precipitate during the high temperature aging process. Since a $SiO_2$–$ZrO_2$ composite has high alkali resistance, it is reasonable that the reverse reaction, dissolution of $SiO_2$ from $SiO_2$–$ZrO_2$, hardly proceeds in the present $ZrO_2$ system [23]. Miller et al. [24] has reported high-surface-area $SiO_2$–$ZrO_2$ prepared by the sol–gel method.

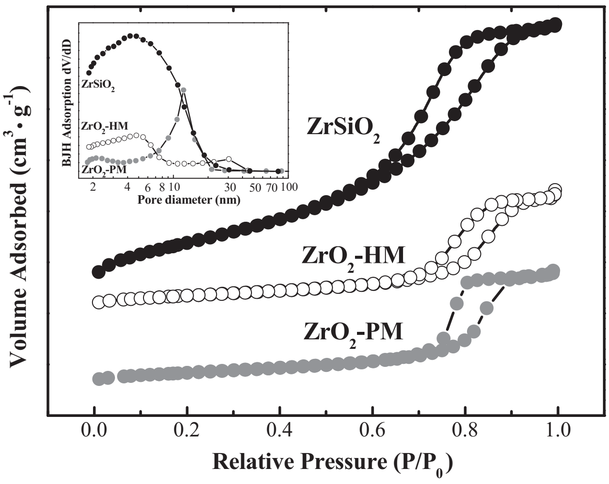

**Fig. 1.** Nitrogen adsorption/desorption isotherms of the $ZrO_2$ and $ZrSiO_2$ supports.

$ZrO_2$ and $ZrSiO_2$ isothermal adsorption–desorption curve was shown in Fig. 1. According to Fig. 1, all the supports calcined at 500 °C for 2 h exhibited type IV adsorption isotherms, associated with capillary condensation taking place in mesopores, and the limiting uptake over a range of high $p/p_0$. The mesoporous texture was also indicated from average pore size (Table 1). According to classification of hysteresis loops from IUPAC [30], they belonged to Type H2 loop, attributed to a difference in mechanism between condensation and evaporation processes occurring in pores with narrow necks and wide bodies, and associated with "ink bottle" pores. The hysteresis hoop of $ZrSiO_2$ was wider than that of $ZrO_2$-PM and $ZrO_2$-HM, which indicated that the pore size distribution of $ZrSiO_2$ was broader than that of PM-$ZrO_2$ and HM-$ZrO_2$.

#### 3.1.2. XRD

The XRD patterns of $ZrO_2$ and $ZrSiO_2$ were shown in Fig. 2. According to Fig. 2, $ZrO_2$ prepared with PM and HM had a good crystal and it belonged to monoclinic crystal, while $ZrSiO_2$ had no obvious characteristic peak and was the amorphous structure. The diffraction peaks of $ZrO_2$-PM were higher than $ZrO_2$-HM. The peaks at 2-Theta = 28.2 and 31.5 corresponded to the (1 1 1) reflection.

#### 3.1.3. TPR and CO chemisorption

TPR profiles of the catalyst was presented in Fig. 3. This clearly suggested that the reduction of ruthenium took place in two forms. In the TPR profile of catalyst, the first peak could be attributed to the reduction of well-dispersed $RuO_x$ or $RuO_2$ particles [31]. It has been found that $RuCl_3$ can be oxidized at the surface by air exposition at room temperature. Moreover, color changes were observed when the $RuCl_3$ impregnated catalysts were exposed upon air, indicating the transformation of the chloride into an oxide and the formation of ruthenium oxychloride [32]. The similar modification was observed in the preparation of Ru/$ZrO_2$ and Ru/$ZrSiO_2$

**Table 1**
BET surface area of the supports and metal dispersion of the catalysts.

| Support | $S_{BET}$ ($N_2$) ($m^2\,g^{-1}$) | Total pore volume ($cm^3\,g^{-1}$) | Average pore diameter (nm) | Silica content (wt.%) | Catalyst | Metal dispersion (%) | Active particle diameter (nm) |
|---|---|---|---|---|---|---|---|
| $ZrO_2$-PM | 60.79 | 0.17 | 9.03 | 0 | Ru/$ZrO_2$-PM | 13.96 | 9.55 |
| $ZrO_2$-HM | 63.77 | 0.17 | 9.16 | 0 | Ru/$ZrO_2$-HM | 14.17 | 9.40 |
| $ZrSiO_2$ | 251.15 | 0.43 | 5.67 | 5.29 | Ru/$ZrSiO_2$ | 21.82 | 6.11 |

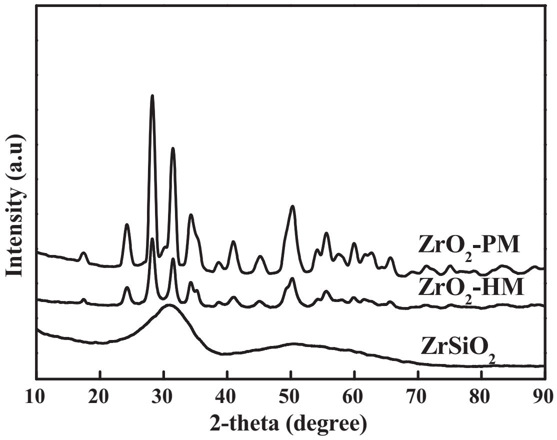

**Fig. 2.** XRD patterns of $ZrO_2$ and $ZrSiO_2$ supports.

catalyst. Another peak may be related with the presence in this catalyst of oxidized ruthenium species strongly interacting with the support or more possibly located in the narrowest pores of the support [31,33]. After the TPR experiments carried out up to 300 °C, the metal dispersion and mean particle diameter were determined by CO chemisorption at 50 °C. The corresponding mean particle diameter was calculated assuming a stoichiometry CO:Ru = 1:1 and a spherical shape of Ru particles. As shown in Table 1, higher Ru dispersion was found for Ru/$ZrSiO_2$.

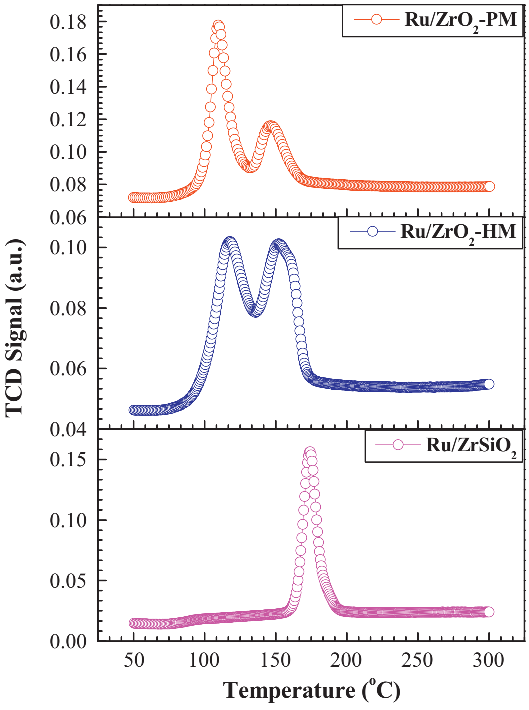

**Fig. 3.** TPR profiles of the catalysts.

### 3.1.4. TEM

As shown in Fig. 4, the TEM image for each catalyst was obtained to find out the particle size of Ru metals for the Ru/$ZrO_2$-PM, Ru/$ZrO_2$-HM and Ru/$ZrSiO_2$ catalysts. In the reports of Wang [34] and Hamzah [35], the Ru loading was 3 wt.% and 5 wt.%, respectively, and the TEM images were able to provide with a clear view of the Ru particles. But it was hard to identify the Ru particle in Fig. 4, which may be because the Ru loading was only 1 wt.% and the Ru particle was too small. The $ZrO_2$ (1 1 1) reflection was found in Ru/$ZrO_2$-PM and Ru/$ZrO_2$-HM.

### 3.1.5. TGA

According to TG–DTG curves in Fig. 5, it indicated that the weight loss stage of $ZrSiO_2$ precursor may be divided into two parts, 100–400 °C and 400–500 °C, respectively. The weight loss of $ZrSiO_2$ precursor was increased rapidly by enhancing temperature from 100 °C to 400 °C, which was because both the adsorbed water and free water were removed. And the weight loss rate (DTG) reached maximum at 160 °C. The weight loss was further produced when the temperature was enhanced from 400 °C to 500 °C. And then the weight of $ZrSiO_2$ was approximately stable.

## 3.2. Effect of supports on catalytic activity of Ru catalysts

Under the reaction conditions of 2000 mg $L^{-1}$ PCP initial concentration, 1.1 MPa oxygen partial pressure and 180 °C, the CWAO experiments were carried out, and the results were shown in Fig. 6(a and b). According to Fig. 6(a), the PCP conversion rate rose with the time moving on. PCP conversion rate reached 79.1% after 30 min over Ru/$ZrSiO_2$ catalyst, while it was only 57.3% and 47.5% over Ru/$ZrO_2$-HM and Ru/$ZrO_2$-PM catalysts, respectively. When the linear fitting was done between $\ln(m_{Ao}/m_{Af})$ and time ($m_{Ao}$: the initial concentration of PCP, $m_{Af}$: PCP concentration in reaction process), it was found that PCP reaction in CWAO obeyed the first order kinetic model [36] and the linear slope was the reaction rate constant $k$ of PCP in CWAO. According to Fig. 6(b), the relationship of catalysts on reaction rate constants was as follows: $k_{Ru/ZrSiO_2} \succ k_{Ru/ZrO_2\text{-HM}} \approx k_{Ru/ZrO_2\text{-PM}}$. Thus, it showed that Ru/$ZrSiO_2$ catalyst had the higher catalytic activity in CWAO, which was because the $ZrSiO_2$ had the higher specific surface area. According to Fig. 6(b), the PCP reaction rate constant $k$ of Ru/$ZrSiO_2$ was 1.6 times larger than that of Ru/$ZrO_2$-PM.

## 3.3. Effect of the calcination temperature of $ZrSiO_2$ precursor on catalytic activity

Under the low temperature and pressure conditions of 180 °C and 0.1 MPa oxygen partial pressure, the effect of the calcination temperature of $ZrSiO_2$ precursor on catalytic activity was studied. The results were shown in Fig. 7. According to Fig. 7(a), the catalytic activity gradually decreased as the calcination temperature increased. According to Fig. 7(b), when the $ZrSiO_2$ precursor was calcined at 400 °C, the reaction rate constant of PCP was twice larger than that of 800 °C. This was because the specific surface area of $ZrSiO_2$ decreased as the calcination temperature went up [22], leading to lower catalytic activity eventually. Although the $ZrSiO_2$ precursor which was calcined at 400 °C and loaded with Ru

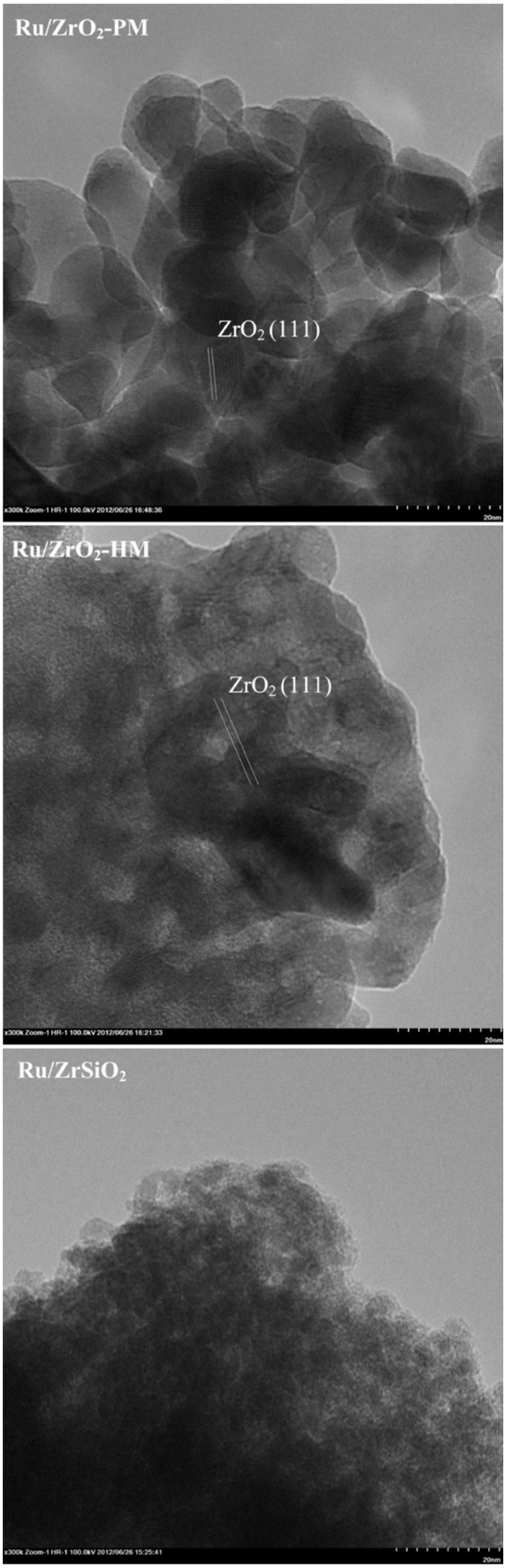

**Fig. 4.** TEM images of the catalysts.

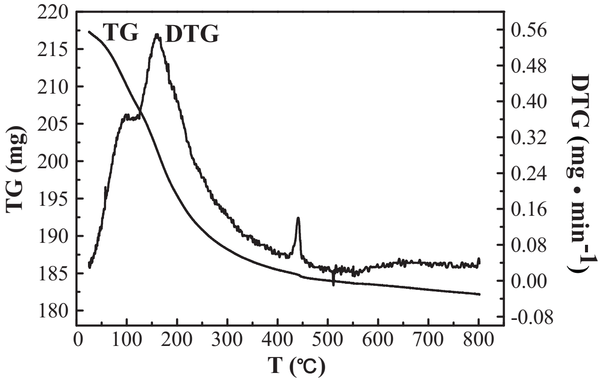

**Fig. 5.** TG–DTG curves of the $ZrSiO_2$ precursor.

possessed the highest catalytic activity, the catalyst broke into powder after the CWAO reaction. According to TGA plot (Fig. 5) of $ZrSiO_2$ precursor, 500 °C was chosen as the best calcination temperature.

### 3.4. Effects of reaction conditions on PCP conversion

#### 3.4.1. Effect of reaction temperature

0.1 MPa oxygen (1.4 times of stoichiometric oxygen demand) was filled into a 250 ml autoclave, and then the effect of different temperature on PCP conversion was studied. The results in Fig. 8(a) showed that the temperature had a great effect on PCP conversion rate. PCP had no obvious conversion at 135 °C and the conversion rate was only 14% after 90 min. As the reaction temperature rose, PCP conversion rate also gradually went up, and it showed an approximate linear relationship. PCP conversion rate reached even 100% at 195 °C. As the temperature rose, PCP molecules in the solution moved more quickly which made the increasing collision and adsorption probability between PCP and the catalytic active site, and then resulting in the high PCP conversion.

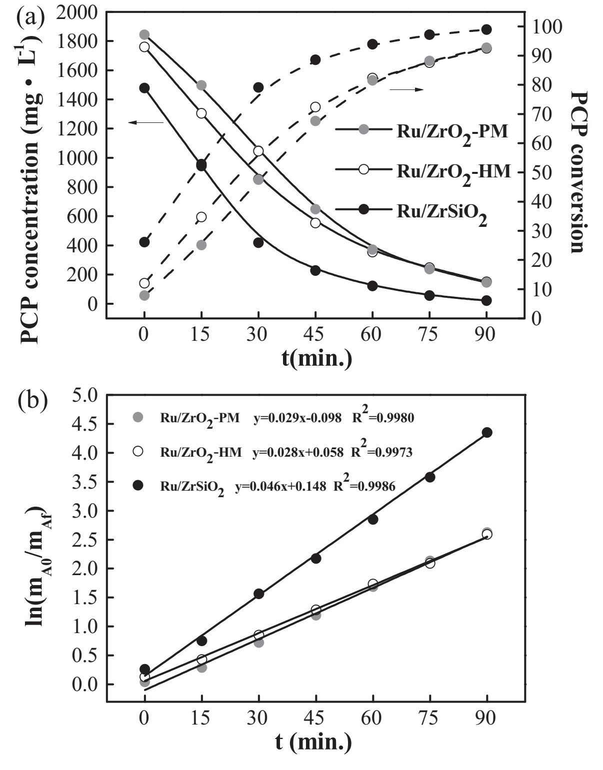

**Fig. 6.** Effect of supports on catalytic activity of Ru catalysts.

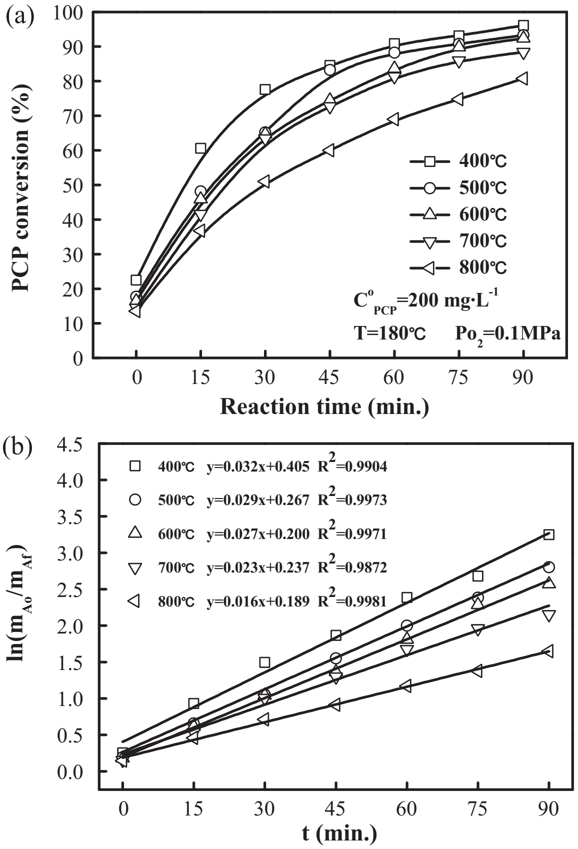

**Fig. 7.** Effects of $ZrSiO_2$ precursor calcination temperature on catalytic activity.

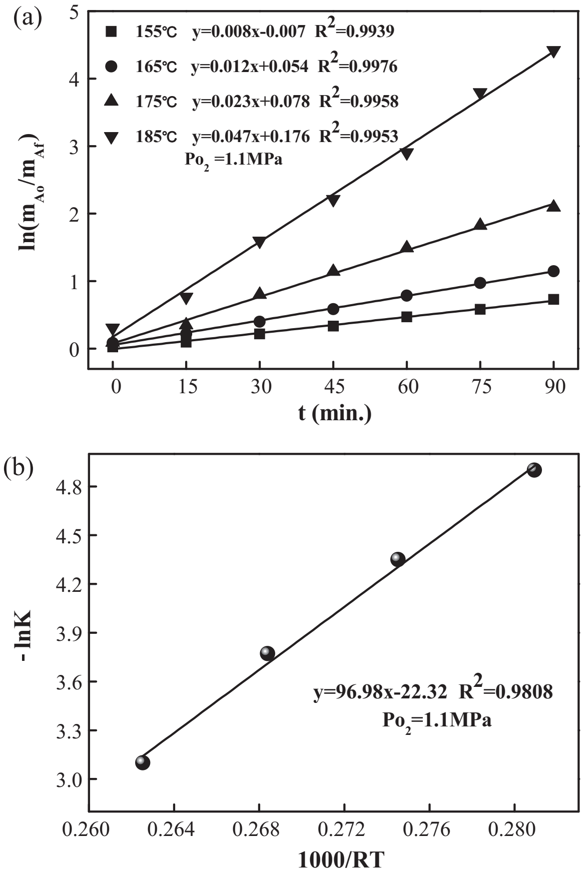

**Fig. 9.** Kinetic plots for PCP in CWAO.

The effect of different reaction temperature on COD removal was studied and the results were shown in Fig. 8(a). According to Fig. 8(a), the temperature also had a great effect on COD removal rate. The removal rate of COD still was 0% at 135 °C after 90 min. As reaction temperature rose, COD removal rate gradually went up. COD removal rate reached only 44% at 195 °C. It may because that the group —H of benzene was substituted by withdrawing electron group —Cl, resulting in the electron density of the benzene ring reducing. So it was not easy for the free radical •OH to attack the benzene ring and very difficult to form aromatic oxygen free radical and open the benzene ring [37], leading to relatively low COD removal rate.

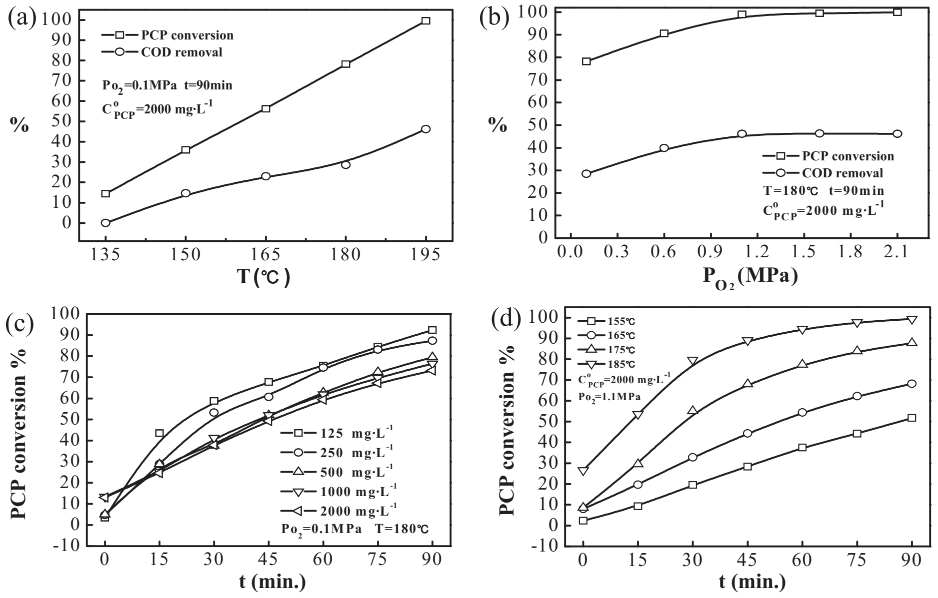

**Fig. 8.** Effect of reaction conditions on PCP conversion and COD removal.

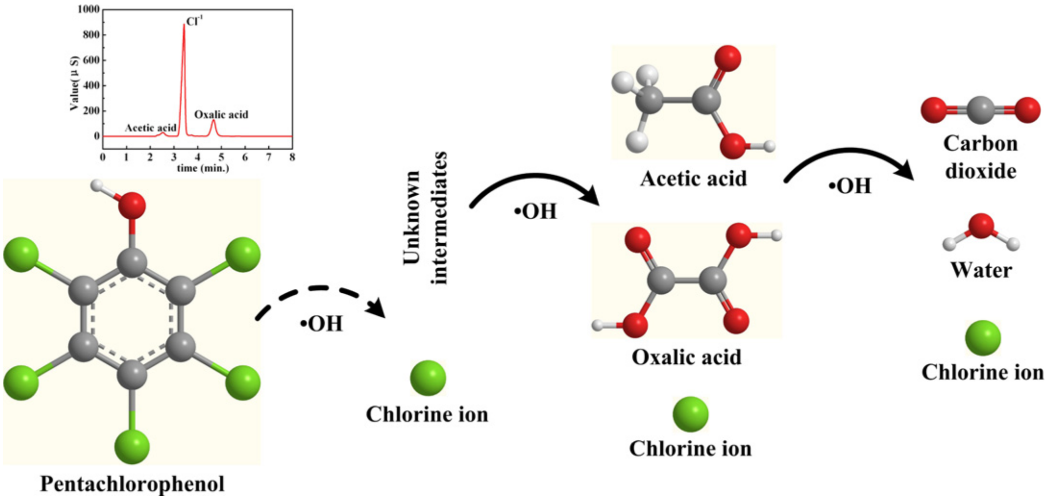

**Fig. 10.** Degradation pathways of PCP in CWAO.

### 3.4.2. Effect of oxygen partial pressure

At 180 °C, the effect of oxygen partial pressure on PCP conversion in CWAO was studied and the results were shown in Fig. 8(b). It indicated that oxygen partial pressure had a relatively great effect on PCP conversion rate when it was less than 1.1 MPa. When oxygen partial pressure was enhanced from 0.1 MPa to 1.1 MPa, the PCP conversion rate was increased by about 20%. This was because as oxygen partial pressure rose, the oxygen concentration in the solution increased according to Henry's law, and then the reaction rate was raised. When oxygen partial pressure reached 1.1 MPa, PCP conversion rate was 99%.

According to the curve between COD removal rate and time in Fig. 8(b), when the oxygen partial pressure was less than 1.1 MPa, it had a relatively great effect on COD removal rate. COD removal rate rose from 28% to 46% when the oxygen partial pressure went up from 0.1 MPa to 1.1 MPa. This was because the rising of oxygen concentration in the solution increased COD removal rate. However, when oxygen partial pressure was more than 1.1 MPa, COD removal rate was not raised any more. The oxygen on the surface of catalyst was saturated and the concentration of the hydroxyl free radial was kept constant. Therefore, higher oxygen partial pressure would not have an effect on COD removal.

### 3.4.3. Effect of initial concentration of PCP

The effect of the initial concentration of PCP on PCP conversion rate was studied under the condition of low oxygen partial pressure of 0.1 MPa. The results were shown in Fig. 8(c). According to Fig. 8(c), during the same reaction time, as the initial concentration of PCP increased, PCP conversion rate gradually decreased. PCP conversion rate was 73% after 90 min when the initial concentration of PCP was 2000 mg $L^{-1}$, while it was 92% when the initial concentration of PCP was 125 mg $L^{-1}$. PCP concentration in the environment was generally lower, so Ru/$ZrO_2$ catalyst prepared with HTAM could degrade most PCP in the environment after 90 min under the conditions of relatively low temperature and pressure.

### 3.4.4. Effect of reaction time

The effect of reaction time on PCP conversion rate was shown in Fig. 8(d). According to Fig. 8(d), PCP conversion rate gradually increased as the reaction time moved on and it reached respectively 68.2% and 99% after 90 min at 165 °C and 185 °C.

Compared with the reaction condition of 165 °C, the kinetic energy of molecules in the solution was relatively larger at 185 °C and the collision probability between PCP and catalyst active site became larger. Therefore, the decomposition of PCP in CWAO became faster.

### 3.5. The study of reaction kinetics on PCP in CWAO

The degradation process of PCP in CWAO may be as follows: PCP was adsorbed to the surface of Ru/$ZrSiO_2$ catalyst and oxidized by the hydroxyl radical $^\bullet$OH produced by oxygen at the catalyst surface. The polyphenols or quinones were gradually produced by the dechlorination reaction of PCP, and then they were mineralized after opening the benzene ring [10]. Acetyl radical $CH_3COO^\bullet$ was formed at the catalyst surface and then underwent a decarboxylation reaction which was usually a slow step. The methyl radicals were eventually oxidized to $CO_2$ [25].

According to the data in Fig. 8(d), the linear fitting was done between $\ln(m_{Ao}/m_{Af})$ and time, and the results were shown in Fig. 9(a). The reaction rate constant $k$ of PCP in CWAO was obtained according to the slope of the fitted line. According to the Arrhenius equation $\ln k = -E_a/RT + \ln A$, the linear fitting was done between $-\ln k$ and 1000/RT. The result in Fig. 9(b) indicated that Arrhenius activation energy of PCP degradation reaction in CWAO was 96.98 kJ $mol^{-1}$.

### 3.6. Degradation pathways of PCP in CWAO

In Fig. 10, only PCP was detected and no other specific peaks were identified in all reaction processes by GC–MS. This may be because the unknown intermediates were very unstable or there was only a little during the reaction processes. The acetic acid, oxalic acid and chlorine ion were identified by IC.

### 3.7. Life evaluation test

Life evaluation test of Ru/$ZrSiO_2$ catalyst was carried out in CWAO, and the results were shown in Fig. 11. The test result indicated that at the reaction conditions of reaction temperature = 180 °C, reaction pressure = 2.0 MPa, catalyst dose = 10 ml, $V_{liquid}$ = 0.33 ml $min^{-1}$ and $V_{gas}$ = 40 ml $min^{-1}$, the PCP conversion was kept essentially constant. The catalyst life was more than 48 h, indicated that the catalyst possessed a high stable performance in CWAO.

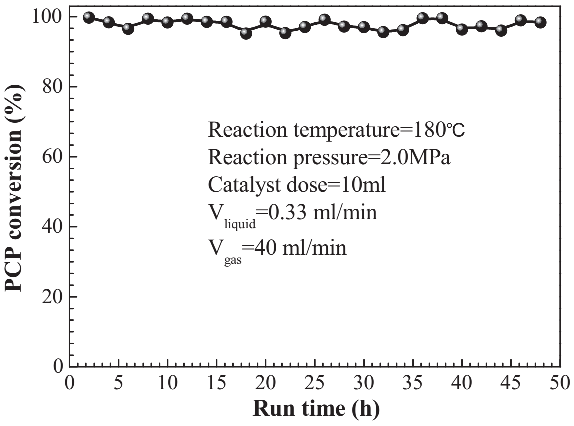

**Fig. 11.** Life evaluation test of Ru/$ZrSiO_2$ catalyst in CWAO.

## 4. Conclusions

In CWAO reaction, it was found that the PCP conversion rate was increased with increasing reaction temperature and oxygen partial pressure, decreasing the initial concentration of PCP and prolonging reaction time. When the drying and calcination conditions were same, the specific surface area of $ZrSiO_2$ was four times higher than that of $ZrO_2$. And the Ru/$ZrSiO_2$ catalyst, which had higher Ru dispersion, exhibited an excellent catalytic activity during the PCP degradation reaction in CWAO. When the initial concentration of PCP was 125 mg L$^{-1}$, PCP conversion reached 92% after 90 min under the low temperature and oxygen partial pressure conditions of 180 °C and 0.1 MPa. According to TGA of $ZrSiO_2$ precursor, 500 °C was chosen as the best calcination temperature. The PCP degradation reaction in CWAO followed the first order kinetic model ($r = kC$). Under the reaction conditions of 180 °C and 1.1 MPa oxygen partial pressure, the Ru/$ZrSiO_2$ catalyst had the largest reaction rate constant of PCP degradation in CWAO and it was 1.6 times larger than that of Ru/$ZrO_2$-PM. Within 48 h, Ru/$ZrSiO_2$ catalyst had a good stability in the fixed-bed reactor with upflow of PCP wastewater and air.

## Acknowledgements

This work was financially supported by Major State Basic Research Development Program of China (No. 2009CB421606), National High-Tech Research and Development Key Program of China (No. 2009AA063903), and Knowledge Innovation Project of the Chinese Academy of Sciences (No. K2009D02).

## References

[1] T.C. Wang, N. Lu, J. Li, Y. Wu, Journal of Hazardous Materials 180 (2010) 436–441.
[2] R. Cheng, W. Zhou, J. Wang, D. Qi, L. Guo, W. Zhang, Y. Qian, Journal of Hazardous Materials 180 (2010) 79–85.
[3] M.A. Salam, R.C. Burk, Water, Air & Soil Pollution 210 (2010) 101–111.
[4] J. Li, G.Z. Qu, N. Lu, G.F. Li, C.H. Sun, Y. Wu, 2009 IEEE Industry Applications Society Annual Meeting, New York, 2009.
[5] Y.C. Chen, C.J. Lin, S.Y. Fu, H.Y. Zhan, Water Science and Technology 61 (2010) 1885–1893.
[6] M.J. Harbottle, G. Lear, G.C. Sills, I.P. Thompson, Journal of Environment Management 90 (2009) 1893–1900.
[7] D.P. Ho, M. Senthilnanthan, J.A. Mohammad, S. Vigneswaran, H.H. Ngo, G. Mahinthakumar, J. Kandasamy, Journal of Advanced Oxidation Technologies 13 (2010) 21–26.
[8] B. Prabowo, B. Veriansyah, J.D. Kim, Journal of Environmental Science 19 (2007) 663–666.
[9] K.H. Hong, S.J. Oh, S.H. Moon, Water, Air & Soil Pollution 145 (2003) 187–203.
[10] J.A. Zimbron, K.F. Reardon, Water Research 43 (2009) 1831–1840.
[11] C.Y. Cui, X. Quan, H.T. Yu, Y.H. Han, Applied Catalysis B-Environmental 80 (2008) 122–128.
[12] W.M. Liu, Y.Q. Hu, S.T. Tu, Journal of Hazardous Materials 179 (2010) 545–551.
[13] S. Zhao, X.H. Wang, M.X. Huo, Applied Catalysis B-Environmental 97 (2010) 127–134.
[14] N. Grosjean, C. Descorme, M. Besson, Applied Catalysis B-Environmental 97 (2010) 276–283.
[15] G.K. Chuah, Catalysis Today 49 (1999) 131–139.
[16] K. Maeda, H. Terashima, K. Kase, M. Higashi, M. Tabata, K. Domen, Bulletin of the Chemical Society of Japan 81 (2008) 927–937.
[17] A. Pintar, M. Besson, P. Gallezot, Applied Catalysis B-Environmental 30 (2001) 123–139.
[18] S.K. Tadokoro, E. Muccillo, Journal of the European Ceramic Society 22 (2002) 1723–1728.
[19] K. Matsui, M. Ohgai, Journal of the American Ceramic Society 85 (2002) 545–553.
[20] C. Stöcker, M. Schneider, A. Baiker, Journal of Porous Materials 2 (1996) 325–330.
[21] M.M. Rashad, H.M. Baioumy, Journal of Materials Processing Technology 195 (2008) 178–185.
[22] S. Jaenicke, G.K. Chuah, V. Raju, Y.T. Nie, Catalysis Surveys from Asia 12 (2008) 153–169.
[23] S. Sato, R. Takahashi, T. Sodesawa, S. Tanaka, K. Oguma, K. Ogura, Journal of Catalysis 196 (2000) 190–194.
[24] J.B. Miller, S.E. Rankin, E.I. Ko, Journal of Catalysis 148 (1994) 673–682.
[25] A. Cybulski, Industrial and Engineering Chemistry Research 46 (2007) 4007–4033.
[26] N. Li, C. Descorme, M. Besson, Catalysis Communications 8 (2007) 1815–1819.
[27] C. Yu, P. Zhao, G. Chen, B. Hu, Applied Surface Science 257 (2011) 7727–7731.
[28] N. Li, C. Descorme, M. Besson, Applied Catalysis B-Environmental 76 (2007) 92–100.
[29] G.K. Chuah, S. Jaenicke, Applied Catalysis A-General 163 (1997) 261–273.
[30] K.S.W. Sing, D.H. Everett, R.A.W. Haul, L. Moscou, R.A. Pierotti, J. Rouquerol, T. Siemieniewska, Pure and Applied Chemistry 57 (1985) 603–619.
[31] V. Choque, P.R.D.L. Piscina, D. Molyneux, N. Homs, Catalysis Today 149 (2010) 248–253.
[32] V. Mazzieri, F. Coloma-Pascual, A. Arcoya, P.C.L. Argentière, Applied Surface Science 210 (2003) 222–230.
[33] C.S. Srikanth, V.P. Kumar, B. Viswanadham, K.V.R. Chary, Catalysis Communications 13 (2011) 69–72.
[34] W. Wang, H. Liu, T. Wu, P. Zhang, G. Ding, S. Liang, T. Jiang, B. Han, Journal of Molecular Catalysis A: Chemical 355 (2012) 174–179.
[35] N. Hamzah, N.M. Nordin, A.H.A. Nadzri, Y.A. Nik, M.B. Kassim, M.A. Yarmo, Applied Catalysis A-General 419 (2012) 133–141.
[36] J.R. Portela Miguelez, J. Lopez Bernal, E. Nebot Sanz, E. Martinez De La Ossa, Chemical Engineering Journal 67 (1997) 115–121.
[37] H.S. Joglekar, S.D. Samant, J.B. Joshi, Water Research 25 (1991) 135–145.